Pergamon

0045-7949(94)E0186-6

Computers & Structures Vol. 58, No. 4, pp. 835–843, 1996
Elsevier Science Ltd
Printed in Great Britain
0045-7949/96 $9.50 + 0.00

COUPLED TORSIONAL–FLEXURAL VIBRATION OF SHAFT SYSTEMS IN MECHANICAL ENGINEERING—I. FINITE ELEMENT MODEL

Qing Hua Qin† and **Cheng Xiong Mao**‡

†Department of Mechanics and ‡Department of Electrical Engineering, Huazhong University of Science and Technology, Wuhan, 430074, People's Republic of China

(*Received* 9 *July* 1993)

Abstract—A new shaft element model with 10 degrees of freedom for coupled torsional–flexural vibration of rotor systems is developed. The model is based on an extended Hamilton's principle and includes the effects of translational and rotational inertia, gyroscopic moments, bending, shear and torsional deformations, internal viscous and hysteretic damping, and mass eccentricity. The practical efficiency of the new element has been assessed through a series of examples.

1. INTRODUCTION

Rotary machines, such as motors, compressors and turbines are very common and widely used. Recently the designers of these machines have been required to meet very severe specifications from the demands of high speed operating power or improvements in efficiency and reliability for the design. In such situations, finding some robust and reliable mathematical models, in conjunction with special numerical solution procedures, which enable designers to make an accurate assessment of the relevant parameters, the critical speeds and the dynamic behaviour of the system, especially the response of the system to unbalance excitation, is of great importance in order to design for increased speeds of rotation, to optimize weight, to improve reliability, and to reduce maintenance costs.

During the last 30 years many different mathematical methods have been proposed for the analysis of rotor systems (see reference lists in Dimarogonas and Paipetis [1] and Zhang [2]). To the authors' knowledge an early work on the use of a finite element method for modelling a rotor-system is due to Ruhl and Booker [3, 4], but their finite element model only includes translational inertia and bending effects. At about the same time Thorkildsen [5] developed a finite element which was more general than Ruhl and Booker's in that it also included rotatory inertia and gyroscopic moments. In 1974 Polk [6] presented a study on natural whirl speed and critical speed analysis using a Rayleigh beam finite element. Nelson and Mcvaugh [7], using the Rayleigh beam theory, improved Polk's model by adding the effects of axial load and axial torque. Gash [8] refined the formulation by taking account of the destabilizing effect due to linear viscous damping. Zorzi and Nelson [9] inspired by the work of Gunter [10] and Dimarogonas [11], include a second destabilizing mechanism due to internal hysteretic damping. Later on Nelson [12] presented a model which included shear deformation but neglected internal damping. Özgüven and Özkan [13], and Hashish and Sankar [14] extended the description of the cylindrical C^1-compatible shaft element by synthesizing the previous models. More recently Edney *et al.* [15] described a conical-C^1 compatible shaft element with eight degrees of freedom, by assuming constant shear distribution along the length of the element, Gmür and Rodrigues [16] developed a set of C^0-compatible linearly tapered shaft elements including the effects of translational and rotatory inertia, gyroscopic moments, internal viscous and hysteretic damping, shear deformation and mass eccentricity, but not including torsional effects. Moreover the excitation is limited to being harmonic (e.g. unbalanced forces).

From the preceding survey of the development of rotor system models an observation may be made. Researchers have in the past focused their attention mainly on the development of rotor system elements including the effects of translational and rotatory inertia, gyroscopic moments, internal viscous and hysteretic damping, shear deformation, and mass eccentricity, and the spin speed is often assumed to be constant. These approaches are inadequate to study dynamic behaviour of a large power system due to a pulse load or other special load. At the same time these formulations are not able to model the coupled torsional-transverse motion, such as the subsynchronous torsional oscillations of steam turbines and generator shaft [17], due to neglecting the torsional deformation. Sometimes it is important to obtain the information concerning the instantaneous coupled torsional and transverse behaviour of a rotor bearing

system, especially for those regions close to the rotor instability conditions. In this case, a time–space finite element model, in which the effects of torsional deformation are also included and the limitation of the spin speed being constant is removed, is required for providing meaningful solutions and for a proper understanding of the dynamic behaviour of a rotor-bearing system.

2. MECHANICAL MODELLING

2.1. *System configuration*

A typical elastic shaft-bearing system to be analysed consists of a shaft, m rigid disks and n linear fluid-film bearings. Such a system is illustrated in Fig. 1. A fixed coordinate reference system (XYZ), with the X-axis coinciding with the undeformed centreline of the shaft, is used to describe the system configuration. The shaft element is considered to be initially straight and is modelled as a 10 degrees of freedom element, namely two translations and three rotations at each end point of the element, while the cross-section of the element, located at a distance s from the left end point, translates and rotates during the general motion of the element. The translational displacements in the Y- and Z-directions of the cross-section centreline, neglecting axial motion, are given by the two displacements (v, w). The rotations of the cross-section about the Y-, Z- and X-axes are described by the rotation angles ($\theta_y = \gamma_y - \partial w/\partial s$, $\theta_z = \partial v/\partial s - \gamma_z$, $\theta_x = \Omega t + \eta$, where γ_y and γ_z are shear strains in the Y- and Z-directions, Ω is the rotational velocity inputting by the electric motor, and η the torsion angle of the shaft which is assumed to be a small parameter).

2.2. *Shape functions*

A two node Timoshenko shaft element with five degrees of freedom at each node is used as a model. Following the method of [2, 18], the translation of a typical point of the element is, in this case, approximated by the relation

$$\begin{pmatrix} v(s,t) \\ w(s,t) \end{pmatrix} = \begin{bmatrix} N^*(s) & 0 \\ 0 & N^*(s) \end{bmatrix}_{2\times 8} \{a_1(t)\}_{8\times 1}, \quad (1)$$

where $\{a_1(t)\}$ and $\{a_2(t)\}$ in (3) are the generalized parameter vectors, and

$$N^*(s) = \{1 \quad s \quad s^2 \quad s^3\}, \quad (2)$$

while the rotation of a typical cross-section of the element is interpolated by

$$\begin{Bmatrix} \theta_y \\ \theta_z \\ \theta_x \end{Bmatrix} = \begin{bmatrix} 0 & 0 & 0 & 0 & 0 & -1 & -2s & -3s^2+6EI/kGA & 0 & 0 \\ 0 & 1 & 2s & 3s^2+6EI/kGA & 0 & 0 & 0 & 0 & 0 & 0 \\ 0 & 0 & 0 & 0 & 0 & 0 & 0 & 0 & 1 & s \end{bmatrix} \begin{matrix} a_1 \\ \\ a_2 \end{matrix}, \quad (3)$$

where E is Young's modulus, G the shear modulus, k the shear correction factor, A the cross-sectional area, and I the second moment of area about a diameter.

The nodal displacements of a typical element are the values of v, w, θ_y, θ_z and θ_x at the ends 1 and 2 of the element (see Fig. 1). Applying the "boundary conditions" to (1) and (3), leads to

$$d = ca \quad (4a)$$

or

$$a = c^{-1}d \quad (4b)$$

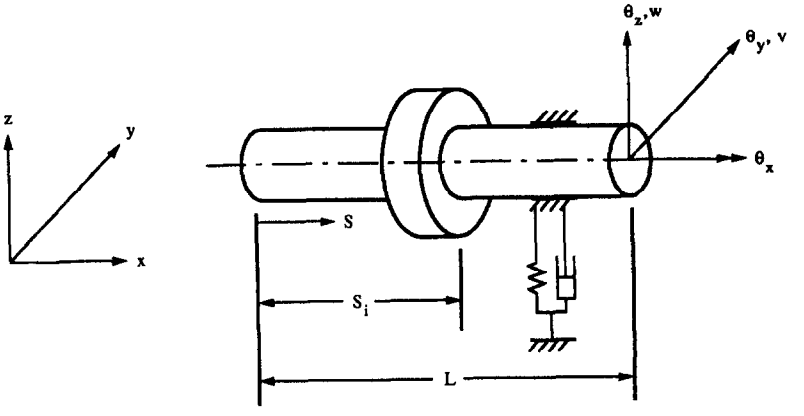

Fig. 1. Typical element and coordinate systems.

$$u(s,t) = Nd, \tag{5}$$

where

$$u(s,t) = \{v \quad w \quad \theta_y \quad \theta_z \quad \theta_x\}^T(s,t) \tag{6}$$

$$d = \{v_1 \quad w_1 \quad \theta_{y1} \quad \theta_{z1} \quad \theta_{x1} \times v_2 \quad w_2 \quad \theta_{yz} \quad \theta_{z2} \quad \theta_{x2}\}^T \tag{7}$$

$$N = \begin{bmatrix} N_1 & 0 & 0 & N_2 & 0 & N_3 & 0 & 0 & N_4 & 0 \\ 0 & N_1 & -N_2 & 0 & 0 & 0 & N_3 & -N_4 & 0 & 0 \\ 0 & D_1 & -D_2 & 0 & 0 & 0 & D_3 & -D_4 & 0 & 0 \\ D_1 & 0 & 0 & D_2 & 0 & D_3 & 0 & 0 & D_4 & 0 \\ 0 & 0 & 0 & 0 & 1-\xi & 0 & 0 & 0 & 0 & \xi \end{bmatrix}, \tag{8}$$

and where $\xi = s/L$, L is the length of the element, and

$$N_1 = (1 + \psi - \psi\xi - 3\xi^2 + 2\xi^3)/(1+\psi)$$

$$N_2 = L\xi(1 + \psi/2 - 2\xi - \psi\xi/2 + \xi^2)/(1+\psi)$$

$$N_3 = (\psi\xi + 3\xi^2 - 2\xi^3)/(1+\psi)$$

$$N_4 = L\xi(-\psi/2 - \xi + \psi\xi/2 + \xi^2)/(1+\psi)$$

$$D_i = \partial N_i/\partial s + (EI/kGA)\partial^3 N_i/\partial s^3$$

$$\psi = 12EI/kGA. \tag{9}$$

2.3. *Finite element formulation*

The element formulation can be derived by use of the extended Hamilton's principle, which states that the true path renders the definite integral

$$H = \int_{t_1}^{t_2} (T - V + W)\,dt \tag{10}$$

stationary with respect to any variation of the path between two instants t_1 and t_2 providing the path variation vanishes at the end points. The equations of motion are thus determined by the relation

$$\int_{t_1}^{t_2} [\delta(T - V) + \delta W]\,dt = 0, \tag{11}$$

where T and V are the kinetic and potential energies respectively of the element and δW represents the variational work done by external forces.

2.3.1. *Rotor element.* The kinetic and strain energies for an isotropic linear elastic beam, including transverse shear and torsional deformations, are given by

$$T^s = (1/2)\int_0^L \{m^s(\dot{v}^2 + \dot{w}^2) + I_d^s(\dot{\theta}_y^2 + \dot{\theta}_z^2) + I_P^s(\dot{\theta}_x^2 - 2\Omega\theta_y\dot{\theta}_z)\}\,ds \tag{12}$$

$$V^s = (1/2)\int_0^L \{EI[(\partial\theta_y/\partial s)^2 + (\partial\theta_z/\partial s)^2] + kGA[(\partial v/\partial s - \theta_z)^2 + (\partial w/\partial s + \theta_y)^2] + GJ(\partial\theta_x/\partial s)^2\}\,ds, \tag{13}$$

in which m^s, I_d^s and I_p^s are, respectively, mass per unit length, dimetral and polar mass moments per unit length, and J is the cross-sectional polar moment of inertia.

The variational work of a typical shaft element is expressed by

$$\delta W^s = \int_0^L \delta U^T \mathbf{P}^s\,ds, \tag{14}$$

where $\mathbf{P}^s = \{q_y\, q_z\, M_y\, M_z\, M_x\}^T$ is the external force vector. If the vector only includes the local unbalance force, $\mathbf{P}^s$ can be further expressed by

$$\mathbf{P}^s \approx \rho A\Omega^2\{e_y^s\cos\Omega t - e_z^s\sin\Omega t,\ e_y^s\sin\Omega t + e_z^s\cos\Omega t,\ 0,\ 0,\ 0\}^T \tag{15}$$

where ρ is mass density, and e_y^s and e_z^s are eccentricities in the Y- and Z-directions of the shaft element.

2.3.2. *Rigid disk.* Assume that a typical rotor element includes n rigid disks which are located at $s_1, s_2, \ldots, s_n$, respectively. The kinetic energy of these disks can be expressed by

$$T^d = (1/2)\sum_i^n \{m_i^d(\dot{v}^2 + \dot{w}^2) + I_{di}^d(\dot{\theta}_y^2 + \dot{\theta}_z^2) + I_{pi}^d(\dot{\theta}_x^2 - 2\Omega\theta_y\dot{\theta}_z)\}_{s=s_i}, \tag{16}$$

while the variational work of these disks is expressed by

$$\delta W^d = \sum_i^n \delta U^T P_i^d|_{s=s_i}, \tag{17}$$

where $P_i^d = \{0\,0\,M_{yi}\,M_{zi}\,M_{xi}\}^T$ for a general loading case, and

$$P^d \approx m_i^d\Omega^2\{e_{yi}^d\cos\Omega t - e_{zi}^d\sin\Omega t,\ e_{yi}^d\sin\Omega t + e_{zi}^d\cos\Omega t,\ 0,\ 0,\ 0\}^T \tag{18}$$

for the unbalance forces, and where m_i^d, I_{di}^d and I_{pi}^d denote the mass, diametrical and polar mass moment

of inertia of disk i, e^d_{yi} and e^d_{zi} are the mass centre eccentricities of disk i in the global Y- and Z-directions. The application of Hamilton's extended principle equation (11), with the energy and work expressions (12)–(17) and interpolation equation (5), produces the following matrix equation of the motion for the shaft–disk element:

$$[M^s + M^d]\{\ddot{d}\} + [G^s + G^d]\{\dot{d}\} + K^s\{d\} = \mathbf{Q}^s + \mathbf{Q}^d \quad (19)$$

where

$$\mathbf{M}^s = \int_0^L N^T \alpha^s N \, ds, \qquad G^s = \int_0^L N^T \beta^s N \, ds, \qquad K^s = \int_0^L B^T \gamma B \, ds$$

$$\mathbf{Q}^s = \int_0^L N^T P^s \, ds, \qquad M^d = \sum_i^n M_i^d, \qquad G^d = \sum_i^n G_i^d$$

$$\mathbf{Q}^d = \sum_i^n Q_i^d, \qquad M_i^d = N^T \alpha_i^d N|_{s=s_i} \qquad G_i^d = N^T \beta_i^d N|_{s=s_i}$$

$$\mathbf{Q}_i^d = N^T P_i^d|_{s=s_i}$$

where

$$\alpha^i = \text{diag}[m^i \quad m^i \quad I_d^i \quad I_d^i \quad I_p^i] \quad (i = s, d)$$

$$\gamma = \text{diag}[\text{kGA} \quad \text{kGA} \quad \text{EI} \quad \text{EI} \quad \text{GJ}]$$

$$B = bN$$

$$\beta^i = \begin{bmatrix} 0 & 0 & 0 & 0 & 0 \\ 0 & 0 & 0 & 0 & 0 \\ 0 & 0 & 0 & I_p^i\Omega & 0 \\ 0 & 0 & -I_p^i\Omega & 0 & 0 \\ 0 & 0 & 0 & 0 & 0 \end{bmatrix}$$

$$b = \begin{bmatrix} \partial/\partial s & 0 & 0 & -1 & 0 \\ 0 & \partial/\partial s & 1 & 0 & 0 \\ 0 & 0 & \partial/\partial s & 0 & 0 \\ 0 & 0 & 0 & \partial/\partial s & 0 \\ 0 & 0 & 0 & 0 & \partial/\partial s \end{bmatrix}$$

and where $[M^s + M^d] = [M]$, $[G^s + G^d] = [G]$, K^s denote the mass, gyroscopic and stiffness matrices of the element, respectively, each being of order 10, while $\mathbf{Q}^s + \mathbf{Q}^d = \mathbf{Q}$ represents the equivalent nodal force vector.

2.3.3. *The effects of internal damping.* During rotation, the element of the rotor, besides contributing to the distributed mass and elastic deformations, the rotating shaft also contributes to the internal damping. Following the procedure of Zorzi and Nelson [9], the constitutive relationship between the moment, shear force, torque and the corresponding strains for a damped shaft element can be, in this case, given by

$$\begin{Bmatrix} M_y \\ M_z \\ M_x \end{Bmatrix} = \begin{bmatrix} EI[\Psi]_{2\times 2} & & 0 \\ & & 0 \\ 0 & 0 & GJF \end{bmatrix} \begin{Bmatrix} \partial\theta_y/\partial s \\ \partial\theta_z/\partial s \\ \partial\theta_x/\partial s \end{Bmatrix} + \begin{bmatrix} EI\Psi_v & 0 & 0 \\ 0 & EI\Psi_v & 0 \\ 0 & 0 & GJ\Psi_v \end{bmatrix} \begin{Bmatrix} \partial\dot{\theta}_y/\partial s \\ \partial\dot{\theta}_z/\partial s \\ \partial\dot{\theta}_x/\partial s \end{Bmatrix} \quad (20)$$

$$\begin{Bmatrix} \mathbf{Q}_y \\ \mathbf{Q}_z \end{Bmatrix} = kGA[\Psi] \begin{Bmatrix} \partial v/\partial s - \theta_z \\ \partial w/\partial s + \theta_y \end{Bmatrix} + kGA \begin{bmatrix} \Psi_v & 0 \\ 0 & \Psi_v \end{bmatrix} \begin{Bmatrix} \partial\dot{v}/\partial s - \dot{\theta}_z \\ \partial\dot{w}/\partial s + \dot{\theta}_y \end{Bmatrix}, \quad (21)$$

where

$$[\Psi] = \begin{bmatrix} F & \\ -(\Psi_v\Omega + \Psi_H/\sqrt{1+\Psi_H^2}) & \Psi_v\Omega + \Psi_H\sqrt{1+\Psi_H^2}) \\ & F \end{bmatrix} \quad (22)$$

$$F = (1 + \Psi_H)\sqrt{1+\Psi_H^2}$$

and where Ψ_v and Ψ_H designate the hysteretic loss factor and viscose damping coefficients, respectively.

By means of the above expressions, the corresponding strain energy and dissipation function may be defined in the form:

$$V^s = (1/2)\int_0^L (EI\{\partial\theta_y/\partial s, \partial\theta_z/\partial s\}[\vartheta] \times \{\partial\theta_y/\partial s, \partial\theta_z/\partial\sigma\}^T + kGA\{\partial v/\partial s - \theta_z, \partial w/\partial s + \theta_y\}[\vartheta]\{\partial v/\partial s - \theta_z, \partial w/\partial s + \theta_y\}^T + GJF(\partial\theta_x/\partial s)^2) \, ds \quad (23)$$

$$D^s = (1/2)\int_0^L [EI\{\partial\dot{\theta}_y/\partial s, \partial\dot{\theta}_z/\partial s\} [\Theta]\{\partial\dot{\theta}_y/\partial s, \partial\dot{\theta}_z/\partial s\}^T$$

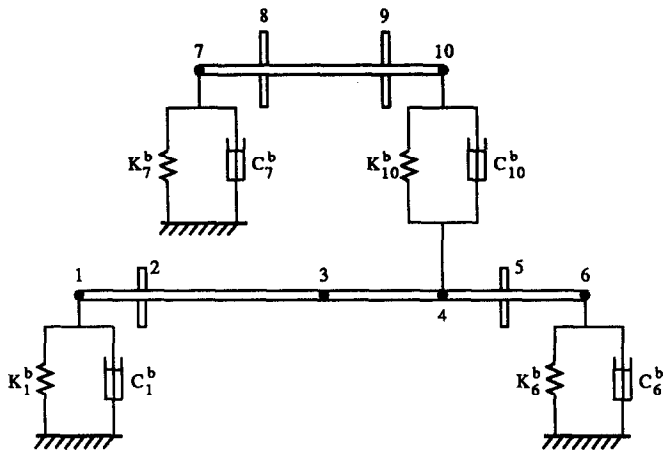

Fig. 2. The configuration of a dual rotor system.

$$+kGA\{\partial v/\partial s-\theta_z,\ \partial w/\partial s+\theta_y\}[\Theta]\{\partial v/\partial s$$

$$-\theta_z,\ \partial w/\partial s+\theta_y\}^{\mathrm{T}}+GJ\Psi_v(\partial\theta_x/\partial s)^2]\,\mathrm{d}s, \quad (24)$$

where $[\Theta]=\mathrm{diag}[\Psi_v, \Psi_v]$.

Thus the Lagrangian equations of motion, including internal damping, of the shaft–disk element can be established as

$$[M]\{\ddot{d}\}+[\Psi_v K^s+G]\{\dot{d}\}$$

$$+[FK^s+K_c(\Psi_v\Omega+\Psi_H/\sqrt{1+\Psi_H^2})]\{d\}=Q, \quad (25)$$

where K_c is a circulation matrix and skew-symmetric:

$$K_c=\int_0^L B^{\mathrm{T}}\lambda B\,\mathrm{d}s \quad (26)$$

$$\lambda=\begin{bmatrix}0 & kGA & 0 & 0 & 0\\ -kGA & 0 & 0 & 0 & 0\\ 0 & 0 & 0 & EI & 0\\ 0 & 0 & -EI & 0 & 0\\ 0 & 0 & 0 & 0 & 0\end{bmatrix}. \quad (27)$$

2.3.4. *The effects of fluid-film bearing.* A satisfactory model for most practical cases is to assume the validity of the usual linearized relationship between the fluid-film forces and the displacements and velocities of the bearing location. In this standard model, the local matrices related to the journal bearings may be expressed as [16]

$$K_L^b=\begin{bmatrix}k_{yy}^b & k_{yz}^b & 0\\ k_{yz}^b & k_{zz}^b & 0\\ 0 & & 0\end{bmatrix}_{5\times 5} \quad (28a)$$

$$C_L^b=\begin{bmatrix}C_{yy}^b & C_{yz}^b & 0\\ C_{yz}^b & C_{zz}^b & 0\\ 0 & 0 & 0\end{bmatrix}_{5\times 5}, \quad (28b)$$

where the stiffness and damping coefficients, which are determined either experimentally or analytically, depend upon the value of the spin speed Ω.

The effects of the journal bearings can, therefore, be directly incorporated into eqn (25) by adding adequate contributions due to K_L^b and C_L^b. If we assume that a typical rotor element includes n linear fluid-film bearings which are located at $s_1, s_2, \ldots, s_n$, respectively, the finite element equation (25) becomes

$$[M]\{\ddot{d}\}+[C]\{\dot{d}\}+[K]\{d\}=Q \quad (29)$$

Table 1. Data of a dual rotor damped system

Station	M (kg)	I_p (kg m^2)	K N/m	C N s/m	L m
1	0.0577	0	2.6269×10^7	5254	0.0762
2	10.7023	0.0859	—	0	0.1778
3	0.2499	0	—	0	0.1524
4	0.1538	0	—	0	0.0508
5	7.0869	0.0678	—	0	0.0508
6	0.0385	0	1.7513×10^7	3502	0.0508
7	0.0467	0	1.7513×10^7	3502	0.0508
8	7.202	0.0429	—	0	0.1524
9	3.692	0.0271	—	0	0.0508
10	0.0467	0	0.8756×10^7	1751	0.0508

$E=2.068\times10^{11}$ N/m^2.

Table 2. Eigenvalues obtained by the present FEM compared with CMS for example 1

Present FEM			CMS		
λ	ω	δ	λ	ω	δ
−1.98	469.2	0.0265	−2.00	469.51	0.0268
−14.08	727.52	0.1216	−14.15	728.33	0.1220
−113.62	1420.98	0.5024	−114.06	1423.34	0.5033
−107.42	2171.69	0.3108	−108.56	2174.93	0.3155
−62.54	2334.03	0.1684	−63.57	2335.42	0.1709
−70.23	3010.93	0.1466	−71.42	3014.76	0.1488
−255.84	4264.67	0.3769	−257.85	4271.58	0.3791
−62.99	5641.77	0.0725	−64.05	5650.71	0.0712

where

$$[C] = \Psi_v[K^s] + [G] + [C^b] \tag{30}$$

$$[K] = F[K^s] + [K_c](\Psi_v\Omega + \Psi_H/\sqrt{1+\Psi_H^2}) + [K^b] \tag{31}$$

$$[K^b] = N^T K_L^b N|_{s=s_i} \tag{32a}$$

$$[C^b] = N^T C_L^b N|_{s=s_i}. \tag{32b}$$

In expressions (29)–(32), all matrices are symmetric with the exception of the gyroscopic term $[G]$ and the circulation terms $[K_c]$ which are skew-symmetric. It can be seen from the expression for $[K]$ that the instabilities resulting from internal damping are characterized. It is also noteworthy that both viscous and hysteretic forms of material damping contribute to the circulation effects, with the viscous form also providing a dissipation term, $\Psi_v K^s\{\dot{d}\}$. Thus the viscous form can provide a stable rotor system providing that this dissipation term dominates. This is achieved when for undamped isotropic supports the spin speed is less than the first forward precessional mode (critical speed).

Finally the solution of eqn (29) is twofold:

(1) The homogeneous solution will give the critical speed of the system.

(2) The dynamic response of the system. The enforced external loads are often of general function of time t. So a time–space finite element formulation has to be developed for treating such a category of problems. In doing this, the Wilson–θ method is utilized in this paper. On the other hand, in the time stepping method the centre is to express the acceleration and velocity in terms of displacement at any given time instant, say t_i:

$$\ddot{d}(t_i) = A(t_i)\mathbf{d}(t_i) + B(t_i) \tag{33}$$

$$\dot{d}(t_i) = C(t_i)\mathbf{d}(t_i) + D(t_i). \tag{34}$$

For the Wilson–θ method, we have

$$A(t_{i+1}) = 6/\theta^2\Delta t^2$$

$$B(t_{i+1}) = -6[\mathbf{d}(t_i) + 6\dot{\mathbf{d}}(t_i) \times \theta\Delta t + 2\ddot{\mathbf{d}}(t_i)\theta^2\Delta t^2/3]/\theta^2\Delta t^2$$

$$C(t_{i+1}) = 3/\theta\Delta t$$

$$D(t_{i+1}) = -3\mathbf{d}(t_i)/\theta\Delta t + 2\dot{\mathbf{d}}(t_i)/3 + \ddot{\mathbf{d}}(t_i)\theta\Delta t/3.$$

The substitution of (33) and (34) into (29), leads to

$$\{[K] + 6[M]/\theta^2\Delta t^2 + 3[C]/\theta\Delta t\}\mathbf{d}(t_i + \theta\Delta t) = \mathbf{Q}(t_i) + \theta[\mathbf{Q}(t_i + \Delta t) - q(t_i)]$$

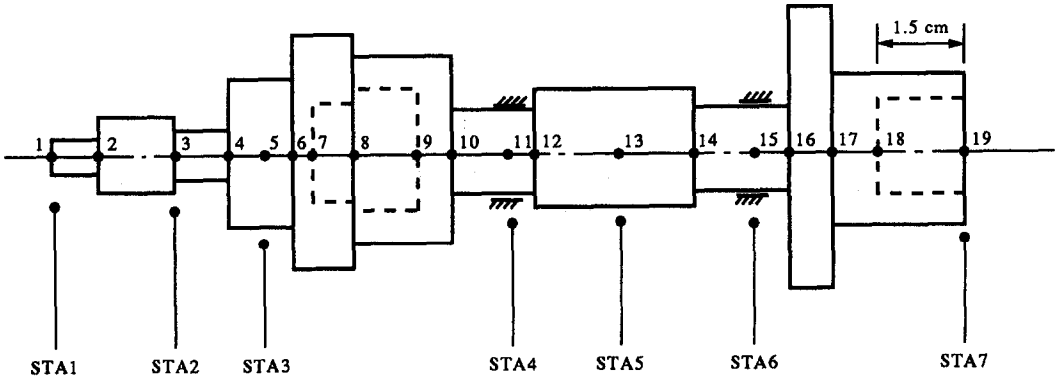

Fig. 3. Rotor configuration for example 2.

Table 3. Initial data for example 2 (cm)

Station	Element	Axial distance to the left end	ID	OD
1	1	0		0.51
	2	1.27		1.02
2	3	5.08		0.76
	4	7.62		2.03
3	5	8.89		2.03
	6	10.16		3.30
	7	10.67	1.52	3.30
	8	11.43	1.78	2.54
	9	12.70		2.54
	10	13.46		1.27
4	11	16.51		1.27
	12	19.05		1.52
5	13	22.86		1.52
	14	26.67		1.27
6	15	28.70		1.27
	16	30.48		3.81
	17	31.50		2.03
	18	34.54	1.52	2.03

Bearing stiffness: $K^b_{yy} = K^b_{zz} = 4.378 \times 10^7$ N/m, $K^b_{yz} = K^b_{zy} = 0$.
Bearing damping: $C^b_{yy} = C^b_{zz} = 2.627 \times 10^3$ N s/m, $C^b_{yz} = C^b_{zy} = 0$.
Hysteretic damping loss factor: $\Psi_H = 0.1$.
Viscous damping coefficients: $\Psi_v = 1.5 \times 10^{-4}$ s.

$$+ [M]\{6\mathbf{d}(t_i)/\theta^2\Delta t^2 + 6\dot{\mathbf{d}}(t_i)/\theta\Delta t + 2\ddot{\mathbf{d}}(t_i)\}$$

$$+ [C]\{3\mathbf{d}(t_i)/\theta\Delta t + 2\dot{\mathbf{d}}(t_i) + \ddot{\mathbf{d}}(t_i)\theta\Delta t/2\}$$

$$(i = 1, 2, \ldots, n), \tag{35}$$

in which θ is a free parameter and the algorithms (33) and (34) are unconditionally stable when $\theta \geqslant 1.37$ (θ is taken to be 1.4 in our paper). Solving (35) we can find the vector $\mathbf{d}$ of the generalized nodal displacements subjected to the initial condition and possibly to some addition essential boundary conditions.

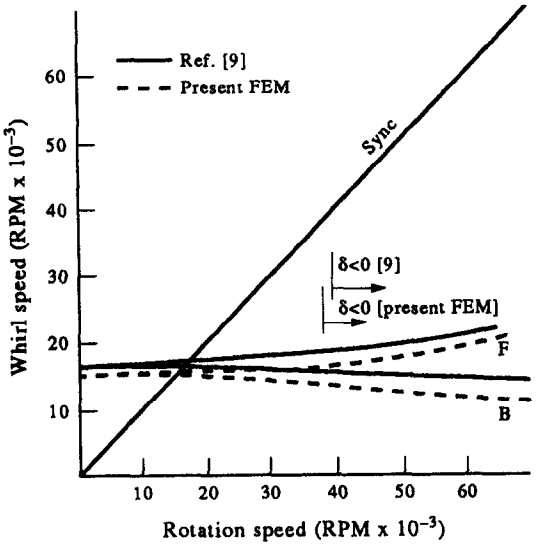

Fig. 4. Whirl speed for example 2.

3. NUMERICAL APPLICATION

The proposed finite element model will be assessed by investigating three examples of rotor systems. In all the calculations, Poisson's ratio is taken to be 0.3. The complex eigenvalues are determined in the form

$$\alpha_i = \lambda_i + i\omega_i \tag{36}$$

and the logarithmic decrement are defined as

$$\delta_i = -2\pi\lambda_i/\omega_i \tag{37}$$

thus the stability region is $\delta_i > 0$.

Example 1. Consider the dual rotor systems [19] shown in Fig. 2. Some initial data are listed in Table 1. The rotating speed and the area moment of inertia about diameter axis of rotor 1 and rotor 2 are 1047.2 rad/s, 2.6467×10^{-9} m^4, 1570.8 rad/s, and 2.1935×10^{-8} m^4, respectively. Table 2 lists the results by the proposed method and comparison is made with that by component mode synthesis (CMS) [19]. It can be seen that those results are in good agreement.

Example 2. Consider a slightly complex rotor system as illustrated in Fig. 3 and investigate its dynamic behaviour and stability with whirl speed. In this example, a density of 7806 kg/cm^2, elastic modulus of 2.075×10^{11} N/m^2 are used for the distributed rotor and a concentrated disk with a mass of 1.401 kg,

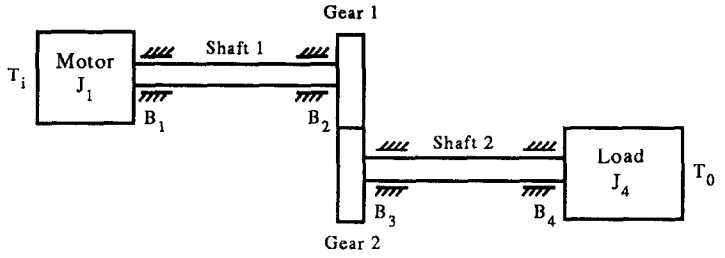

Fig. 5. Model of a single stage spur-gear system.

Table 4. Parameters of the gear system [20]

Tooth profile	STD
Diametrical pitch	4
Number of teeth, Gear 1	20
Number of teeth, Gear 2	20
Pressure angle (°)	20
Pitch radius, Gear 1 (mm)	63.5
Pitch radius, Gear 2 (mm)	63.5
Base radius, Gear 1 (mm)	59.67
Base radius, Gear 2 (mm)	59.67
Face width, (mm)	25.4
Contact ratio	1.56
Backlash (mm)	0.25
Moment of inertia, Drive (kg · m^2)	0.026
Moment of inertia, Load (kg · m^2)	0.026
Moment of inertia, Gear 1 (kg · m^2)	0.0051
Moment of inertia, Gear 2 (kg · m^2)	0.0051
Shaft stiffness, shaft 1 (N · m/rad)	102.0
Shaft stiffness, shaft 2 (N · m/rad)	102.0
Load per unit face width (N/mm)	175

polar inertia of 0.0020 kg/m^2 and diametric inertia of 0.0135 kg/m^2 is located at station 3. As was done in [9], the rotor is modelled by 18 elements which are listed in Table 3. The numerical results are shown in Fig. 4. It can be seen from Fig. 4 that the present value of damped critical speed (16,950 rpm) is slightly lower than that of Zorzi and Nelson [9] (17,500 rpm). The main reason is due to the effects of shear- and torsional-deformation.

Example 3. The example reproduces the results presented by Kumar and Sanker [20] of the spur gear system shown in Fig. 5. The detailed information on the system physical properties contained in [20] is reproduced in Table 4. The integration time step is taken to be 0.2 s. Figure 6 shows the relative response of a gear pair and comparison is made with those given by Kumar and Sankar [20]. The results demonstrate that the proposed method can treat time varying shaft system.

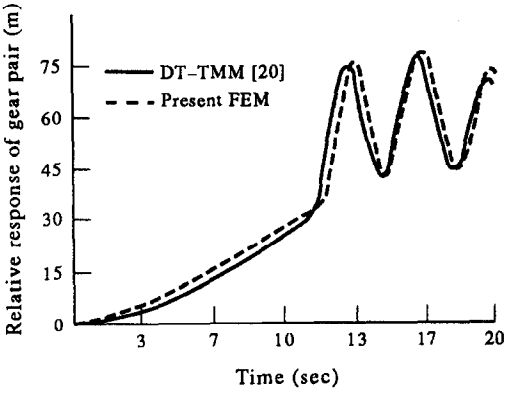

Fig. 6. Relative response of the gear pair modelled.

4. CONCLUSION

A new shaft element model with 10 degrees of freedom is developed for calculating critical speed and for the dynamic response analysis of a rotor system. The proposed method is based on an extended Hamilton's principle. It includes the effects of translational and rotational inertia, gyroscopic moments, bending-, shear- and torsional-deformations, internal viscous and hysteretic damping, and mass eccentricity. The numerical effort in this study included three practical examples and the results indicate that the finite element model developed in this paper provides an accurate representation of coupled torsional-flexural dynamic behaviour of a damped shaft system. Moreover the model can be incorporated easily in existing computer programs.

Acknowledgements—The financial support of the national education committee foundation for scholars returning from abroad and the national Natural Science Foundation of China is gratefully acknowledged.

REFERENCES

1. A. D. Dimarogonas and S. A. Paipetis, *Analytical Methods of Rotor Dynamics*. Applied Science Publishers, London (1983).
2. W. Zhang, *Introduction to Rotor Dynamics*. Scientific Press of China, Beijing (1990) (in Chinese).
3. R. L. Ruhl, Dynamics of distributed parameter rotor systems: transfer matrix and finite element techniques. Ph.D. dissertation, Cornell University (1970).
4. R. L. Ruhl and J. F. Booker, A finite element model for distributed parameter turborotor systems. *ASME J. Engng Ind.* **94**, 128–132 (1972).
5. T. Thorkildsen, Solution of a distributed mass and unbalanced rotor system using a consistent mass matrix approach. MSE Engineering Report, Arizona State University, June (1974).
6. S. R. Polk, Finite element formulation and solution of flexible rotor-rigid disc systems for natural frequencies and critical whirl speed. MSE Engineering Report, Arizona State University (May, 1974).

7. H. D. Nelson and J. M. Mcvaugh, The dynamics of rotor bearing systems using finite elements. *ASME J. Engng Ind.* **98,** 593–600 (1976).
8. R. Gash, Vibration of large turbo-rotors in fluid-film bearings on an elastic foundation. *J. Sound Vibr.* **47,** 53–73 (1976).
9. E. S. Zorzi and H. D. Nelson, Finite element simulation of rotor bearing systems with internal damping. *ASME J. Engng Power* **99,** 71–76 (1977).
10. E. J. Gunter, The influence of internal friction on the stability of high speed rotors. *ASME J. Engng Ind.* **89,** 683–688 (1967).
11. A. D. Dimarogonas, A general method for stability of rotating shafts. *Ingenieur-Archiv* **44,** 9–20 (1975).
12. H. D. Nelson, A finite rotating shaft element using Timoshenko beam theory. *ASME J. Mech. Design* **102,** 793–803 (1980).
13. H. N. Özgüven and Z. L. Özkan, Whirl speeds and unbalance response of multibearing rotors using finite elements. *ASME J. Vibr. Acoust., Stress, Reliab. Des.* **106,** 72–79 (1984).
14. E. Hashish and T. S. Sankar, Finite element and modal analysis of rotor bearing systems under stochastic loading conditions. *ASME J. Vibr. Acoust., Stress, Reliab. Des.* **106,** 80–89 (1984).
15. S. L. Edney, C. H. J. Fox and E. J. Williams, Tapered Timoshenko finite elements for rotor dynamics analysis. *J. Sound Vibr.* **137,** 463–481 (1990).
16. T. C. Gmür and J. D. Rodrigues, Shaft finite elements for rotor dynamics analysis. *ASME J. Vibr. Acoust.* **113,** 482–493 (1991).
17. Y. N. Yu, *Electric Power System Dynamics.* Academic Press, New York (1983).
18. D. C. Thomas, J. M. Wilson and R. R. Wilson, Timoshenko beam finite elements. *J. Sound Vibr.* **81,** 315–330 (1973).
19. T. P. Huang, The transfer matrix impedance coupling method for the eigensolutions of multi-spool rotor systems. *ASME J. Vibr. Acoust., Stress, Reliab. Des.* **110,** 468–472 (1988).
20. A. S. Kumar and T. S. Sankar, A new transfer matrix method for response analysis of large dynamic systems. *Comput. Struct.* **23,** 545–552 (1986).